

How to Cite:

Hantosh, A. M., Rajab, N. A., & Abachi, F. T. (2022). Synthesis and antimicrobial activity of new 1,2,3,4-tetrahydropyrimidine-5-carbonyl glycinate silver nanoparticle derivatives. *International Journal of Health Sciences*, 6(S6), 8930–8948.
<https://doi.org/10.53730/ijhs.v6nS6.12375>

Synthesis and antimicrobial activity of new 1,2,3,4-tetrahydropyrimidine-5-carbonyl glycinate silver nanoparticle derivatives

Ali Majeed Hantosh

Department of Pharmaceutical Chemistry

*Corresponding author email: amh_phd@yahoo.com

Nawal A. Rajab

Department of Pharmaceutics, College of Pharmacy, University of Baghdad, Baghdad, Iraq

Email: dr.nawalayash@copharm.uobaghdad.edu.iq

Faris T. Abachi

Department of Pharmaceutical Chemistry, College of Pharmacy, University of Mosul, Mosul, Iraq

Email: farisabachi@yahoo.com

Abstract---A series of silver nanoparticle (AgNPs) with 1,2,3,4 tetrahydropyrimidine derivatives were synthesized and elucidate their structures using physical and spectroscopic techniques (UV.VIS, FTIR, NMR, X-ray diffraction, and SEM). Each of these novel compounds produced spectroscopic data that matched the suggested structures. Pathogenic bacteria and *C.albicans* were used as test subjects for the antimicrobial activity by using agar well diffusion assay. The AgNPs agents show intermediate activity antimicrobial activities as compare with ciprofloxacin as positive control.

Keywords---tetrahydropyrimidine, biginelli multi-component reaction, Sliver nanoparticle, Scanning Electron Microscopy, antimicrobial.

Introduction

Microbial pathogens, such as bacteria, are the primary cause of potentially fatal infectious diseases. To overcome the inhibitory and bactericidal effects of antimicrobial medicines, bacterial pathogens have evolved a number of techniques (1). As a result, it is critical to conserve effective antimicrobials for as long as feasible while continuing to use them to benefit human and animal health (2). Current antibacterial treatments have grown less effective, if not ineffective, as

a result of resistance development. Recently, several approaches of addressing antibiotic resistance have been presented. One potential way for achieving this aim is to combine additional molecules with failed drugs, which appears to restore proper antibacterial action (3). The development of methods to synthesis of nanoparticle heterocyclic compounds and their biological evaluation are important points in organic pharmaceutical and medical chemistry (4). Pyrimidine is a unique (six-membered) heterocyclic ring with two nitrogen atoms. Pyrimidine and tetrahydropyrimidine derivatives were found in many pharmaceutical products with a wide of activities such as antimicrobial (5), anticancer (6), and anticonvulsant (7). Tetrahydropyrimidines can inhibit dihydrofolate reductase (DHFR), which is a potential therapeutic target in antimicrobial research. Regardless of the fact that DHFR is not a novel target, there is a great deal of interest in developing DHFR inhibitors, particularly for mycobacteria (8). Silver nanoparticles has good antimicrobial activity with free of adverse effects relatively (9). AgNPs have various and concurrent modes of action and when combined with antimicrobial agents like antibiotics or organic compounds they enhance their antimicrobial activity (10). In this work we synthesize new DHPM derivatives by Biginelli multi-component reaction that involves the condensation of cyanoethylacetate, substituted aromatic aldehyde and urea or thiourea. The final compounds that we synthesized were conjugated with sAgNPs to give synergistic effect against different microbes.

Experimental work

Commercially available starting materials used without additional purification. By using Stuart Scientific electrothermal apparatus melting points were measured. Fourier transforms Infrared spectroscopy (FTIR) were recorded potassium bromide disks KBr by Shimadzu FTIR 8400S device. ¹HNMR spectra were recorded on 500 MHz Agilent spectrometer using tetra methyl silane (TMS) as an internal standard and dimethyl sulfoxide (DMSO-d₆) as a solvent. Thin-layer chromatography was used to examine the purity (TLC Silica gel 60 F254, Merck, Germany). R_f values determined by TLC with two mobile phases: A- Ethyl acetate/n-hexane (3:7); B- Chloroform: Ethanol (85: 15). Various analytical techniques, including scanning electron microscopy (SEM), UV-VIS spectroscopy and X-ray diffractometry are employed to characterize the produced silver nanoparticles. The synthesized compounds are illustrated by scheme 1.

Chemistry

General procedure of preparation 1,2,3,4-(tetrahydropyrimidine-5-carbonitrile) derivatives [1a-1d]

A mixture of ethyl cyanoacetate (0.03 mol.), various substituted aromatic aldehydes (0.03 mol.) and urea/ thiourea (0.03 mol.) were put in a round-bottomed flask then dissolved in (25 ml) of absolute ethanol that containing (0.01mol.) of K₂CO₃. The mixture was then reflux at (80-100) °C for (8 to 12) hours. The precipitate of the potassium salt that is formed during the reaction was adding to distilled water then acidified with diluted CH₃COOH. The precipitate of the compound was filtered and washed with D.W. then recrystallized with ethanol (11&12). The, physical parameters, R_f values, percent yield and melting point results are listed in Table (1).

Synthesis of 1,2,3,4-(tetrahydropyrimidine-5-carboxylic acid) derivatives [2a-2d]

In (15 ml) of 70% sulfuric acid we dissolve (0.01 mol.) of compounds (1a-1d) and refluxed for 3 hours with heating. The reaction mixture was allowed to cool, then poured onto ice and neutralized with NH_4OH . The desired acid derivatives were obtained by filtering, drying, and recrystallizing the precipitate from ethanol (13&14).

General procedure for synthesis of final compound [3a-3d]

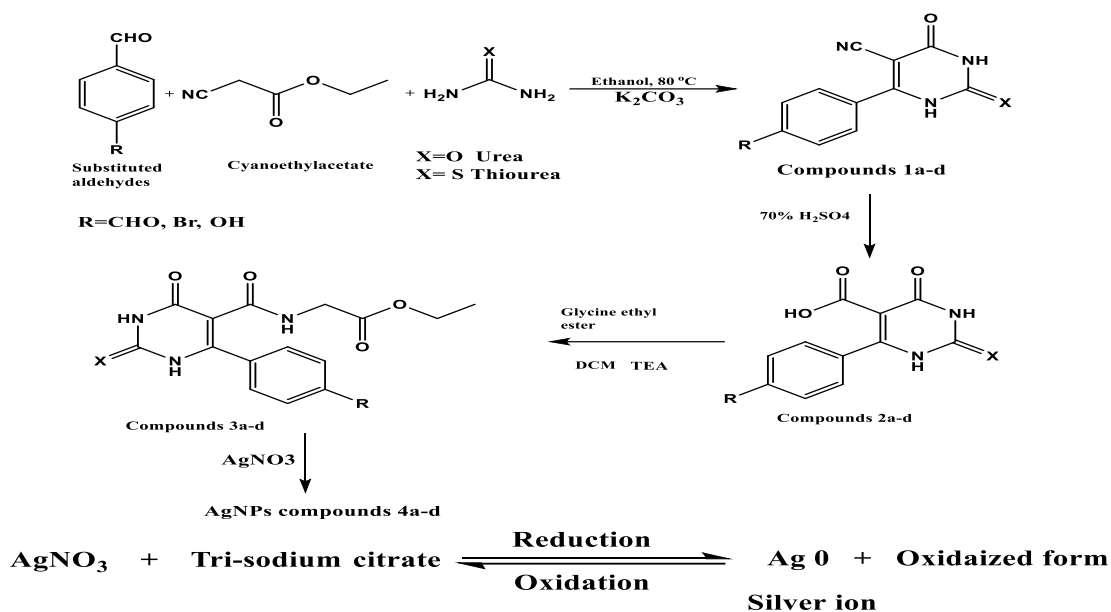
The carboxylic acid compounds [1a-h] (0.01 mol) in 50 ml DCM, then TEA (0.012 mol.) was added to form a clear solution. The solution is chilled in an ice bath to -50 degrees Celsius, after that ethyl chloroformate (0.012 mol.) is added slowly with continuous stirring and left for 25-30 minutes on the magnetic stirrer. The heat of the mixture was kept below 0°C . The Glycine ethyl ester (10 mmol) was dissolved in 0.01L of DCM then added slowly to the chilled mixture while swirling continuously. The combination was left for one hour in the ice bath and keeps it with continuous stirring for 20 hours. Then 3 hours of reflux were conducted. The resultant mixture was placed into a separator funnel and rinsed three times with 5% sodium bicarbonate, 5% HCl solution three times, and finally washed with D.W. three times. The organic layer was then dehydrated with MgSO_4 , and The crude precipitating product was recovered and cleaned with 40-60% petroleum ether, n-hexan, and lastly pure material was produced by recrystallization from ethanol using a rotary evaporator (15).

Synthesis of silver nanoparticales [AgNPs] using Tri-sodium citrate

The molecular synthesis of AgNPs was performed using Silver Nitrate (AgNO_3) plus Trisodium Citrate, and the method is given here. A water bath was used to heat a 100 ml of (1.50 mM) AgNO_3 solution to 90°C throughout 5 minutes. By dropping 12.5 mL of the prepared TSC solution (1.50 percent) was added while constantly swirling. The reduction phase started with a shift in appearance from translucent to pale yellow, indicating the creation of Ag NPs. The nanoparticle mixture was swirled for 20 minutes at 90°C on a stirrer before being kept in a fridge (8°C) for additional stability testing (16,17&18).

Procedure to synthesis of Pyrimidine-AgNPs and Ciprofloxacin-Silver Nanoparticals [4a-4d]

Weigh 0.001 mole of the synthesized Compounds [3a-3d] and the reference compound (Ciprofloxacin) then dissolve in 10 mL distilled water, stirring until complete dissolve. Add dilute HCl for dissolving. Mix 1:1 ratio of Sliver Nanopartical with Compounds. Heat at 95°C for 15 min. Centrifuge for 10-15 min., take the ppt (Pyrimidine -AgNPs). All products are identified by their physical properties and ultraviolet spectroscopy technique (19).



Scheme 1. Synthesis of Silver nanoparticles tetrahydropyrimidine derivatives

Biological Assay

Antimicrobial by using agar well diffusion assay

The antibacterial efficacy of the synthesized samples (4a-4d) was investigated against (Gram's negative and Gram's positive) bacterial strains using agar well diffusion assay while the antifungal activity was investigated against *Candida albicans* (20&21). Aseptically, 20 mL of Muller–Hinton (MH) agar was put into sterile Petri dishes. Using a sterile wire loop, the bacterial species were gathered from their stock cultures (22). On the agar plates, 6 mm-diameter holes were drilled using a sterile needle after the organisms had been cultured. In the bored wells, varied concentrations of the Samples (4a-d) were utilized. Plates containing Samples (4a-d) and test organisms were incubated at 37°C for one night prior to measuring and recording the average diameter of the zones of inhibition (23&24).

Statistical analysis

Data were statically analysis using Graphpad prism program (25). Data are represented as mean \pm SD of three experiments. Indicate statistically significant difference at $p < 0.05$ (26).

Results and Discussion

The physical parameters, R_f values, percent yield and melting point results for the intermediates and final products are listed in Table (1). The (FT-IR) spectra, ^1H NMR and ^{13}C NMR are explained as follow:

Table 1

The physical parameters, R_f values, percent yield and melting point results for the intermediates and final products

Compounds and intermediates	Molecular formula	Molecular weight	Description	Yield %	Melting point °C	R_f value
1a	C ₁₂ H ₇ N ₃ O ₂ S	229	White Pink powder	84	254-257	A=0.79 B=0.32
1b	C ₁₁ H ₇ N ₃ O ₂ S	245	Pale yellow powder	86	250-252	A=0.78 B=0.36
1c	C ₁₁ H ₆ BrN ₃ OS	308	Brown powder	81	247-249	A=0.82 B=0.51
1d	C ₁₁ H ₆ BrN ₃ O ₂	292	Pale Orange powder	78	233-235	A=0.80 B=0.35
2a	C ₁₂ H ₈ N ₂ O ₄ S	276	Pale yellow powder	57	224-226	A=0.73 B=0.36
2b	C ₁₁ H ₈ N ₂ O ₄ S	264	Pale brown powder	56	213-216	A=0.81 B=0.30
2c	C ₁₁ H ₇ BrN ₂ O ₃ S	327	Brown powder	40	207-210	A=0.76 B=0.28
2d	C ₁₁ H ₇ BrN ₂ O ₄	311	Pale brown powder	38	219-221	A=0.78 B=0.30
3a	C ₁₆ H ₁₅ N ₃ O ₅ S	361	White powder	54	184-185	A=0.46 B=0.68
3b	C ₁₅ H ₁₅ N ₃ O ₅ S	349	Pale white powder	61	177-179	A=0.42 B=0.60
3c	C ₁₅ H ₁₄ BrN ₃ O ₄ S	412	Pale yellow white powder	55	175-177	A=0.33 B=0.54
3d	C ₁₅ H ₁₄ BrN ₃ O ₅	396	White powder	57	157-159	A=0.32 B=0.59

Ethyl-6-(4-formylphenyl)-4-oxo-2-thioxo-(1,2,3,4-tetrahydropyrimidine-5-carbonyl) glycinate (1a)

IR cm⁻¹: 3367 (NH stretching of amide), 3180 (NH for pyrimidine ring), 3039 (C-H stretching), 1718 (C=O stretching of ester), 1663 (C=O stretching of amide), 1523 (C=C aromatic stretching). ¹H-NMR (500 MHz, DMSO-d₆): 12.01 (singlet, 1H, NH, N3 pyrimidine ring), 11.88 (singlet, 1H, NH, N1 pyrimidine ring), 9.92 (singlet, for CHO proton of aromatic), 8.48 (Singlet, for NH proton of amide), 7 (Doublet, for CH protons of aromatic ring), 6.71 (Doublet, for CH protons of aromatic ring), 4.01 (Quartet, for CH₂ protons), 3.80 (Singlet, for CH₂ protons of glycine), 1.10 (Triplet, for CH₃ protons of glycine). ¹³C-NMR (100 MHz, DMSO-d₆): 186.11, 134.55, 128.09, 115.58, 144.93, 165.68, 174.31, 157.33, 101.56, 166.97, 54.01, 169.22, 59.94, 14.48.

Ethyl-6-(4-hydroxyphenyl)-4-oxo-2-thioxo-(1,2,3,4-tetrahydropyrimidine-5-carbonyl) glycinate (3b)

IR cm^{-1} : 3487 (O-H stretching), 3448 (NH stretching of amide), 3248&3178 (NH for pyrimidine ring), 3016 (C-H stretching), 1681 (C=O stretching of ester), 1643 (C=O stretching of amide), 1577 (C=C aromatic stretching). $^1\text{H-NMR}$ (500 MHz, DMSO-d_6): 10.36 (singlet, 1H, NH, N3 pyrimidine ring), 10.32 (singlet, 1H, NH, N1 pyrimidine ring), 9.67 (singlet, for HO proton of aromatic), 8.57 (Singlet, for NH proton of amide), 7.40 (Doublet, for CH protons of aromatic ring), 7.22 (Doublet, for CH protons of aromatic ring), 3.99 (Quartet, for CH_2 protons), 3.67 (Singlet, for CH_2 protons of glycine), 1.20 (Triplet, for CH_3 protons of glycine). $^{13}\text{C-NMR}$ (100 MHz, DMSO-d_6): 157.33, 115.58, 128.08, 122.91, 163.49, 174.31, 165.64, 101.55, 151.03, 54.01, 168.52, 59.93, 14.48.

Ethyl-6-(4-bromophenyl)-4-oxo-2-thioxo-(1,2,3,4-tetrahydropyrimidine-5-carbonyl) glycinate (3c)

IR cm^{-1} : 3228 (NH stretching of amide), 3209 (NH for pyrimidine ring), 3109 (C-H stretching), 2962 (C-H stretching), 1724 (C=O stretching of ester), 1697 (C=O stretching of amide), 1516 (C=C aromatic stretching). $^1\text{H-NMR}$ (500 MHz, DMSO-d_6): 12.63 (singlet, 1H, NH, N3 pyrimidine ring), 12.07 (singlet, 1H, NH, N1 pyrimidine ring), 8.20 (Singlet, for NH proton of amide), 7.98 (Doublet, for CH protons of aromatic ring), 6.92 (Doublet, for CH protons of aromatic ring), 4.26 (Quartet, for CH_2 protons), 3.42 (Singlet, for CH_2 protons of glycine), 1.27 (Triplet, for CH_3 protons of glycine). $^{13}\text{C-NMR}$ (100 MHz, DMSO-d_6): 122.58, 134.50, 129.51, 129, 163.17, 176.76, 155.04, 96.85, 164.09, 44.78, 168.94, 62.32, 14.51.

Ethyl-6-(4-bromophenyl)-2,4-dioxo-(1,2,3,4-tetrahydropyrimidine-5-carbonyl) glycinate (3d)

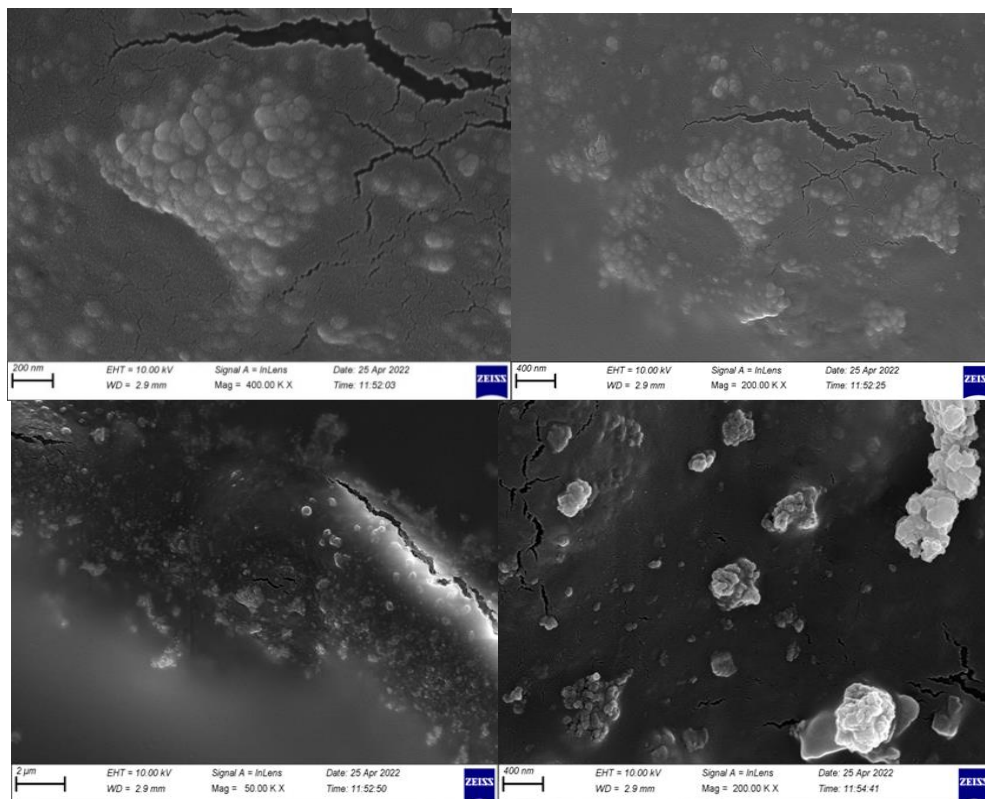
IR cm^{-1} : 3325 (NH stretching of amide), 3170 (NH for pyrimidine ring), 3101 (NH for pyrimidine ring), 2966 (C-H stretching), 1743 (C=O stretching of ester), 1670 (C=O stretching of amide), 1573 (C=C aromatic stretching). $^1\text{H-NMR}$ (500 MHz, DMSO-d_6): 11.95 (singlet, 1H, NH, N3 pyrimidine ring), 10.84 (singlet, 1H, NH, N1 pyrimidine ring), 8.26 (Singlet, for NH proton of amide), 7.97 (Doublet, for CH protons of aromatic ring), 6.94 (Doublet, for CH protons of aromatic ring), 4.29 (Quartet, for CH_2 protons), 3.98 (Singlet, for CH_2 protons of glycine), 1.26 (Triplet, for CH_3 protons of glycine). $^{13}\text{C-NMR}$ (100 MHz, DMSO-d_6): 122.58, 134.50, 129.51, 129, 163.17, 176.76, 155.04, 96.85, 164.09, 44.78, 168.94, 62.32, 14.51.

Characterization of the synthesized Ag nanoparticles

Several analytical methods are used to characterize the produced silver nanoparticles, including scanning electron microscopy (SEM), X-ray diffractometry (XRD) and UV-vis spectroscopy.

Scanning Electron Microscopy (SEM)

Lately, the area of the nano-science and nano-technology had presented the driving force in developing a variety of the techniques of high-resolution microscopy for the purpose of learning more about the nano-materials with the use of highly energetic electron beam in order to probe objects on various fine scales (27, 28&29). Amongst the variety of the techniques of electron microscopy, the SEM is the one with surface imaging, entirely able to resolve various sizes of the particle, nanomaterial shapes, size distributions, and surface morphology of synthesized nano-particles as well as micro-scales (30, 31&32). Through utilizing the SEM, we have the ability of probing morphology of the particles and deriving histogram from images either through the measurement and counting of particles in a manual way, or through the use of certain software (29). SEM results image has shown that rather uniform and spherical Ag NPs have been formed with 26 to 70nm diameter as shown in figure (1). The SEM image shows hydrogel materials with some nanoparticles are immersed in between the hydrogel folds and the nanoparticles are enhanced the nanoparticles present in the hydrogel material. The particles seem as clusters distributed homogeneously between the hydrogel materials. Larger particles of silver could be a result of aggregation of smaller particles, because of measurements of SEM (33).



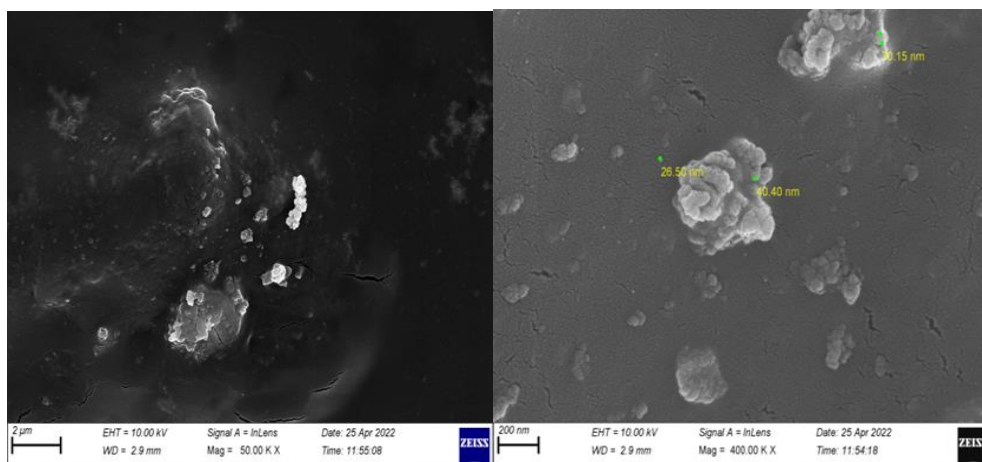


Figure 1. SEM micrograph of the synthesized AgNPs

X-Ray Diffraction Studies

Structural characteristics of phase composition, crystallographic Ag NPs orientation have been additionally characterized with the use of the XRD (34&35). The X-ray diffraction chart shows five main peaks along the 2 theta axes which are representing the silver nanoparticles present in the tested sample. The most intensive peak is of 250 counts, appear at (38.369 °A.) with 100% cystallinity percentage and has 16nm crystal size. The identified peaks [10.92, 20.435, 38.369, 44.458, 68.098], had shown synthesized particles' crystalline nature (Figure2). The result of the XRD has been found to be in accordance with standards of ICSD No98-018-0878 (36&37). In addition to the other four peaks of less crystalline, where all represent the main peaks of the silver nanoparticles as shown in figure (2) and table (2).

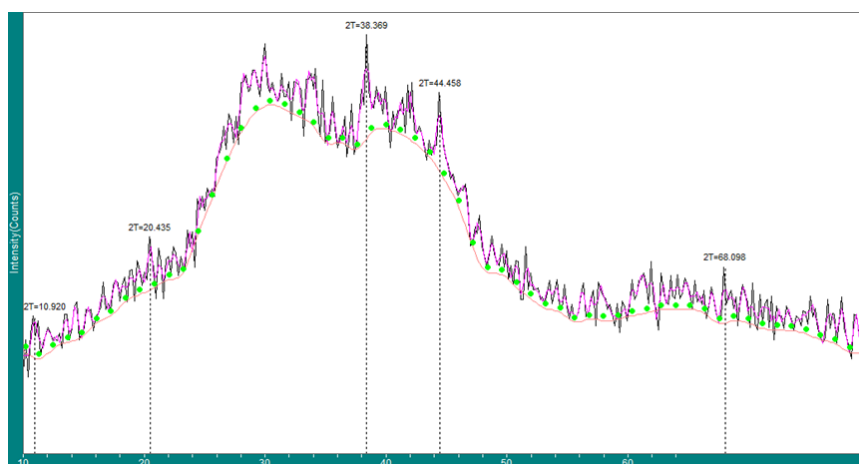


Figure 2. analysis of the synthesized silver nanoparticles using X-ray diffraction (XRD)

Table 2
XRD results of AgNPs

2-Theta	d(nm)	BG	Height	I%	Area	I%	FWHM	crystal Size XS(nm)
10.92	0.80951	76	33	39.8	83	32.9	0.428	19
20.435	0.43424	129	43	51.8	187	74.2	0.739	11
38.369	0.2344	250	83	100	252	100	0.516	16
44.458	0.20361	225	62	74.7	218	86.5	0.598	14
68.098	0.13757	103	45	54.2	139	55.2	0.525	18

UV – VIS spectra result of silver nanoparticles and DHPM compounds coated with AgNPs

Figure (3a-d), illustrates UV-VIS spectra of absorption of Ag NPs and the DHPM@Ag NPs. In an Ag NPs case, as can be seen from Fig. 3a, the spectrum of the absorption of prepared Ag NPs of SPR (i.e. Surface Plasmon Resonance) band of the Ag NPs has appeared about 412nm which has been considered characteristic to Ag NPs formation (38). Following the functionalization, the Ag NPs with the DHPM (3a) there was a shifting in absorption peak that appear at 354 nm as shown in Figure 3a, the appearance of distinct band at longer wave-length 432nm has been considered as one of the vital features proving changes in colour from the yellow to the green, which indicates assembly of the particles. For compound (3b) with Ag NPs the appearance of two distinct band at 348 and 409 nm. The first peak due to the molar absorptivity of the compound (3b) while the second peak is for AgNPs as shown in Figure 3b. For compound (3c) as shown in the figure 3c, the absorption spectra at 337 nm and after functionalization there was a decrease in intensity of AgNPs peak at around 410 nm. The last DHPM compound (3d) as shown in figure 3d show three peaks, two peaks belong for compound (3d) that absorbs at 282 nm and after functionalization with AgNPs there was a decrease in SPR of AgNPs at 409 nm.

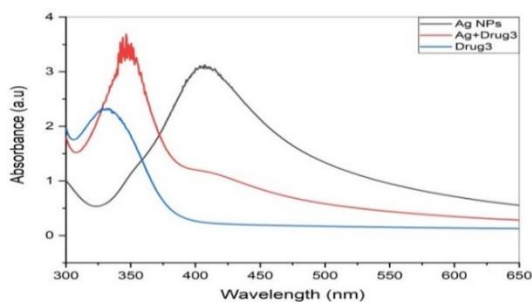


Figure 3a. The AgNPs, compound (3a), and compound (3a) with AgNPs absorption spectra

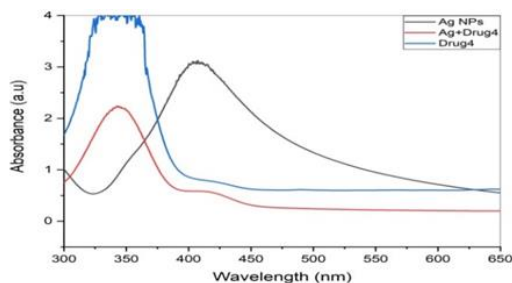


Figure 3b. The AgNPs, compound (3b), and compound (3b) with AgNPs absorption spectra

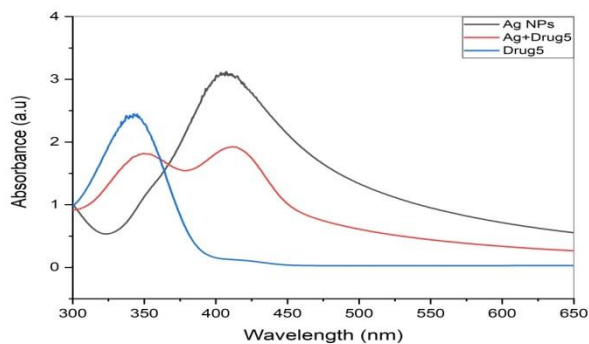


Figure 3c. The AgNPs, compound (3c), and compound (3c) with AgNPs absorption spectra

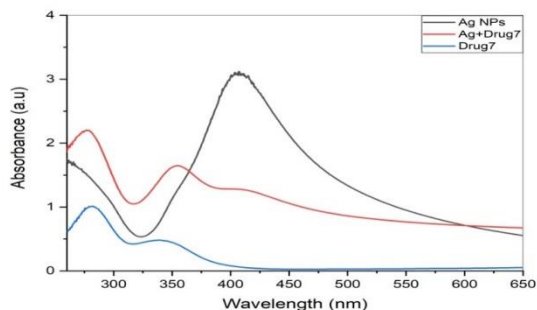


Figure 3d. The AgNPs, compound (3d), and compound (3d) with AgNPs absorption spectra

Biological Activity

Antimicrobial Activity

The synthesized DHPM and Ag NPs were tested against three pathogenic bacteria and one fungi for the antimicrobial efficacy *in-vitro* comparison with Ciprofloxacin as a control, which resulted in varying zones of inhibition at different concentration indicating their antimicrobial properties. All the DHPM@Ag NPs compounds (4a-d) have been found to show very good inhibition of growth for all

the four tested microbes. Compound (4a, 4b and 4c) has been found to have the best inhibition against *Streptococcus pyogenes* at least concentration used $62.5 \mu\text{g/ml}$, while compounds (4d) show intermediate activity in comparison with Ciprofloxacin, as shown in the figures below. The compounds (4a, 4b, 4c and 4d) have almost the same activity as Ciprofloxacin, as shown in the figures below. Compounds (4a and 4c) show the best antibacterial activity against *E.coli* in comparison with the reference Ciprofloxacin also at minimum concentration used. The antifungal activity of the prepared compounds was investigated against *Candida albicans* and all compounds show excellent activity in comparison with the reference drug. The results, in general, indicate that the combination of Ag NPs with the compounds have antimicrobial activity serves as better antimicrobial agents due to synergistic action. The significant antimicrobial effect of the synthesized compounds may be attributable to their capacity to infiltrate the bacterial cytoplasm and even cross the nuclear envelope. Additionally, they may bind to other kinds of enzymes, such as dihydrofolate reductase, aminoacyl-tRNA synthetases, bacterial DNA gyrase, etc (39).

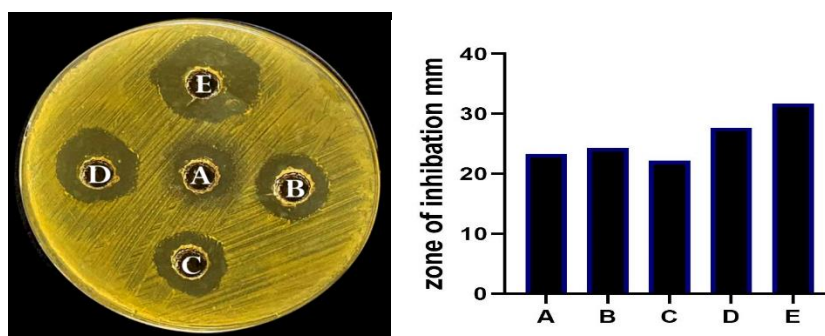


Figure 4. Antibacterial activity of (compound 4a) against *Streptococcus pyogenes*. A, control (Cip $250 \mu\text{g/ml}$). B, bacterial strain treated at concentration $62.5 \mu\text{g/ml}$. C, bacterial strain treated at concentration $125 \mu\text{g/ml}$. D, bacterial strain treated at concentration $250 \mu\text{g/ml}$ E, bacterial strain treated at concentration $500 \mu\text{g/ml}$

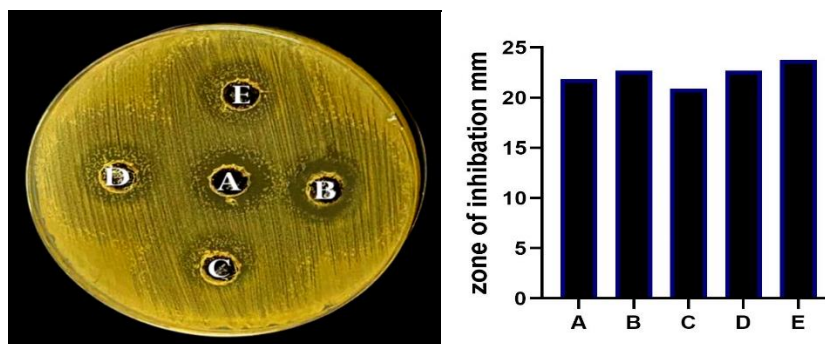


Figure 5. Antibacterial activity of (compound 4b) against *Streptococcus pyogenes*. A, control (Cip $250 \mu\text{g/ml}$). B, bacterial strain treated at concentration $62.5 \mu\text{g/ml}$. C, bacterial strain treated at concentration $125 \mu\text{g/ml}$. D, bacterial strain treated at concentration $250 \mu\text{g/ml}$ E, bacterial strain treated at concentration $500 \mu\text{g/ml}$

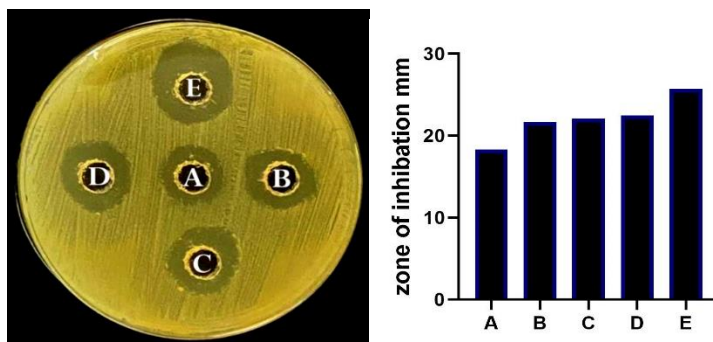


Figure 6. Antibacterial activity of (compound 4c) against *Streptococcus pyogenes*. A, control (Cip 250 $\mu\text{g/ml}$). B, bacterial strain treated at concentration 62.5 $\mu\text{g/ml}$. C, bacterial strain treated at concentration 125 $\mu\text{g/ml}$. D, bacterial strain treated at concentration 250 $\mu\text{g/ml}$. E, bacterial strain treated at concentration 500 $\mu\text{g/ml}$

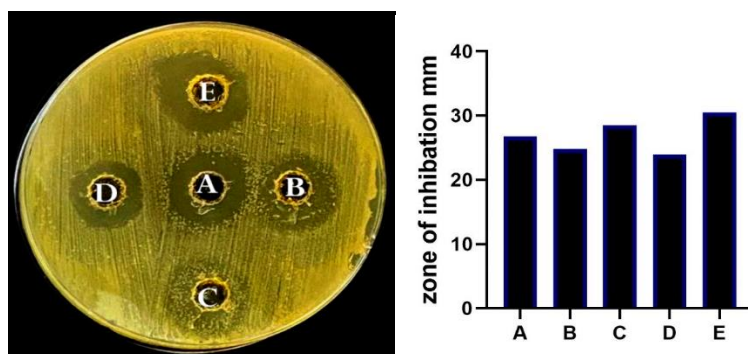


Figure 7. Antibacterial activity of (compound 4d) against *Streptococcus pyogenes*. A, control (Cip 250 $\mu\text{g/ml}$). B, bacterial strain treated at concentration 62.5 $\mu\text{g/ml}$. C, bacterial strain treated at concentration 125 $\mu\text{g/ml}$. D, bacterial strain treated at concentration 250 $\mu\text{g/ml}$. E, bacterial strain treated at concentration 500 $\mu\text{g/ml}$

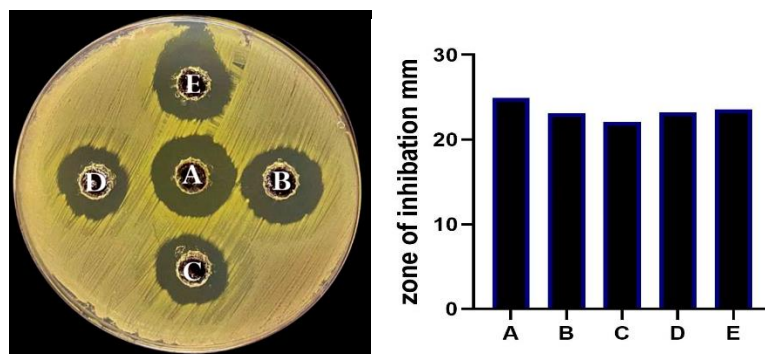


Figure 8. Antibacterial activity of (compound 4a) against *Pseudomonas aeruginosa*. A, control (Cip 250 $\mu\text{g/ml}$). B, bacterial strain treated at concentration 62.5 $\mu\text{g/ml}$. C, bacterial strain treated at concentration 125 $\mu\text{g/ml}$. D, bacterial strain treated at concentration 250 $\mu\text{g/ml}$. E, bacterial strain treated at concentration 500 $\mu\text{g/ml}$

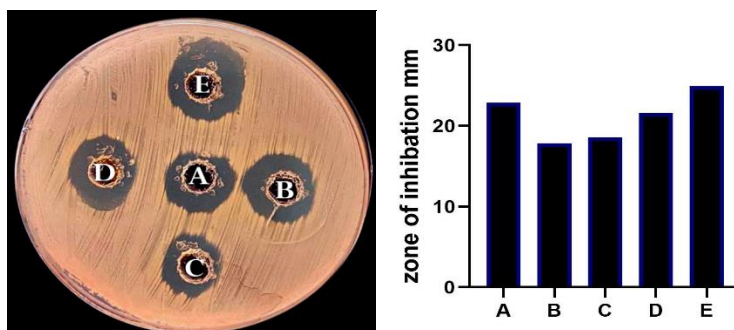


Figure 9. Antibacterial activity of (compound 4b) against *Pseudomonas aeruginosa*. A, control (Cip 250 µg/ml). B, bacterial strain treated at concentration 62.5 µg/ml . C, bacterial strain treated at concentration 125 µg/ml. D, bacterial strain treated at concentration 250 µg/ml. E, bacterial strain treated at concentration 500 µg/ml

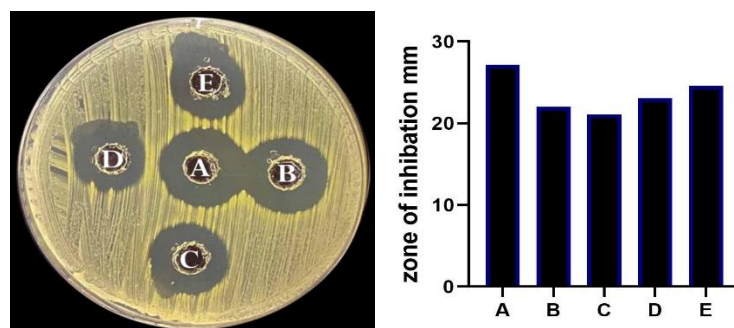


Figure 10. Antibacterial activity of (compound 4c) against *Pseudomonas aeruginosa*. A, control (Cip 250 µg/ml). B, bacterial strain treated at concentration 62.5 µg/ml . C, bacterial strain treated at concentration 125 µg/ml. D, bacterial strain treated at concentration 250 µg/ml. E, bacterial strain treated at concentration 500 µg/ml

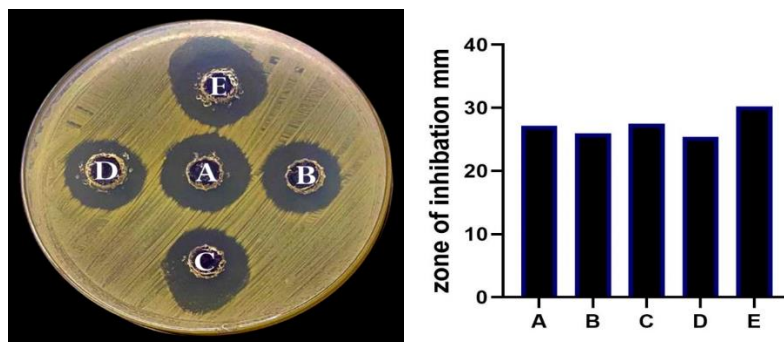


Figure 11. Antibacterial activity of (compound 4d) against *Pseudomonas aeruginosa*. A, control (Cip 250 µg/ml). B, bacterial strain treated at concentration 62.5 µg/ml . C, bacterial strain treated at concentration 125 µg/ml. D, bacterial strain treated at concentration 250 µg/ml. E, bacterial strain treated at concentration 500 µg/ml

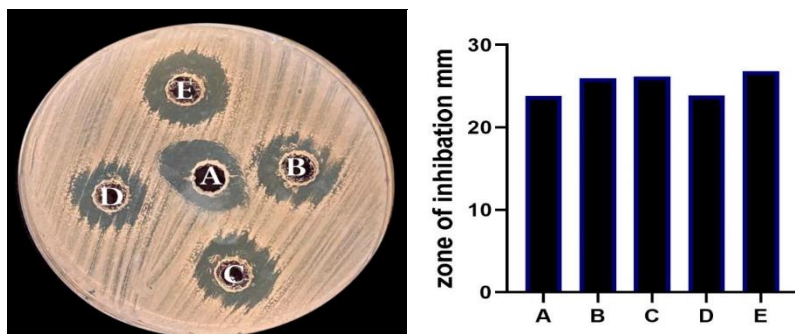


Figure 12. Antibacterial activity of (compound 4a) against *E. coli*. A, control (Cip 250 $\mu\text{g/ml}$). B, bacterial strain treated at concentration 62.5 $\mu\text{g/ml}$. C, bacterial strain treated at concentration 125 $\mu\text{g/ml}$. D, bacterial strain treated at concentration 250 $\mu\text{g/ml}$. E, bacterial strain treated at concentration 500 $\mu\text{g/ml}$

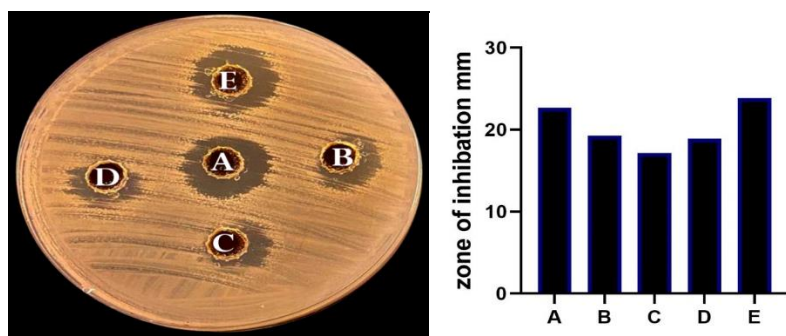


Figure 13. Antibacterial activity of (compound 4b) against *E. coli*. A, control (Cip 250 $\mu\text{g/ml}$). B, bacterial strain treated at concentration 62.5 $\mu\text{g/ml}$. C, bacterial strain treated at concentration 125 $\mu\text{g/ml}$. D, bacterial strain treated at concentration 250 $\mu\text{g/ml}$. E, bacterial strain treated at concentration 500 $\mu\text{g/ml}$

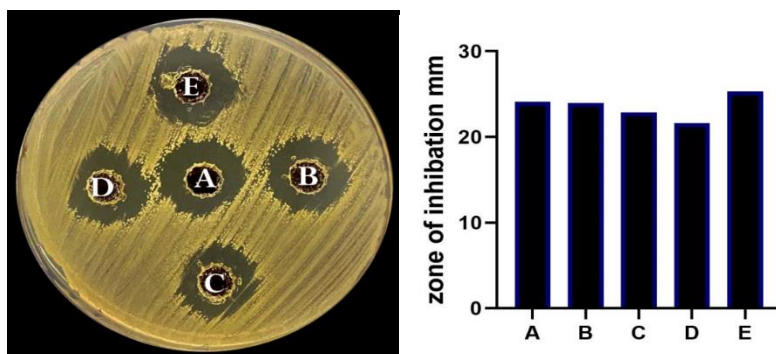


Figure 14. Antibacterial activity of (compound 4c) against *E. coli*. A, control (Cip 250 $\mu\text{g/ml}$). B, bacterial strain treated at concentration 62.5 $\mu\text{g/ml}$. C, bacterial strain treated at concentration 125 $\mu\text{g/ml}$. D, bacterial strain treated at concentration 250 $\mu\text{g/ml}$. E, bacterial strain treated at concentration 500 $\mu\text{g/ml}$

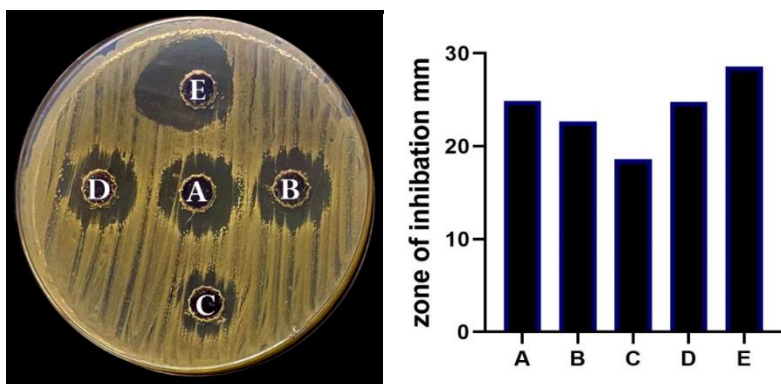


Figure 15. Antibacterial activity of (compound 4d) against *E. coli*. A, control (Cip 250 $\mu\text{g/ml}$). B, bacterial strain treated at concentration 62.5 $\mu\text{g/ml}$. C, bacterial strain treated at concentration 125 $\mu\text{g/ml}$. D, bacterial strain treated at concentration 250 $\mu\text{g/ml}$. E, bacterial strain treated at concentration 500 $\mu\text{g/ml}$

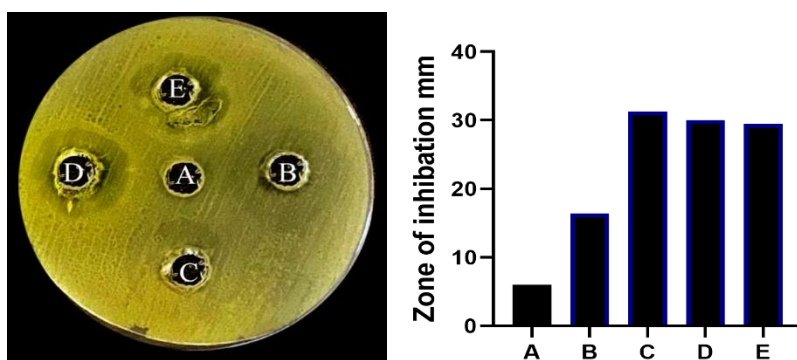


Figure 16. Antifungal activity of (compound 4a) against *Candida albicans*. A, control. B, treated at concentration 62.5 $\mu\text{g/ml}$. C, treated at concentration 125 $\mu\text{g/ml}$. D, treated at concentration 250 $\mu\text{g/ml}$, E, treated at concentration 500 $\mu\text{g/ml}$

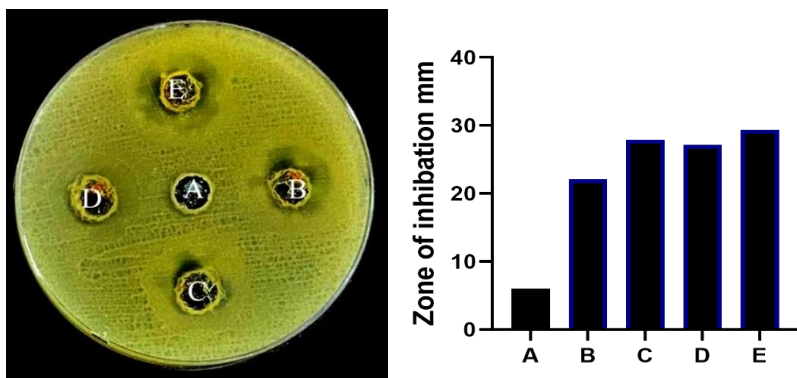


Figure 17. Antifungal activity of (compound 4b) against *Candida albicans*. A, control. B, treated at concentration 62.5 $\mu\text{g/ml}$. C, treated at concentration 125 $\mu\text{g/ml}$. D, treated at concentration 250 $\mu\text{g/ml}$, E, treated at concentration 500 $\mu\text{g/ml}$

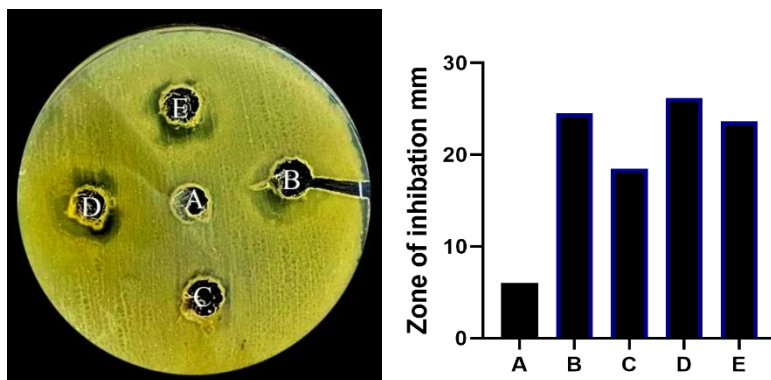


Figure 18. Antifungal activity of (compound 4c) against *Candida albicans*. A, control .B, treated at concentration 62.5 $\mu\text{g/ml}$. C, treated at concentration 125 $\mu\text{g/ml}$. D, treated at concentration 250 $\mu\text{g/ml}$, E, treated at concentration 500 $\mu\text{g/ml}$

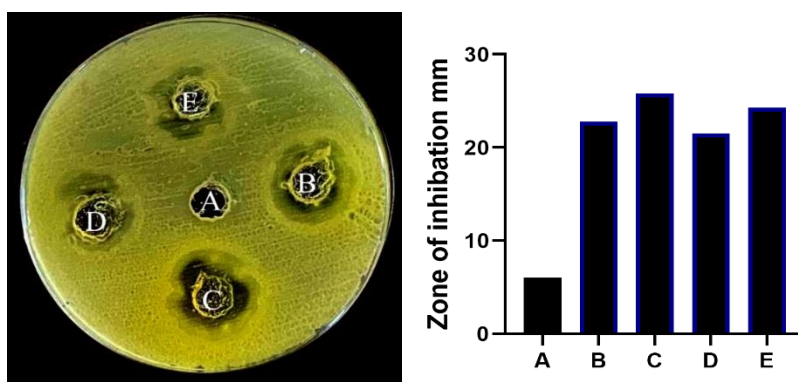


Figure 19. Antifungal activity of (compound 4d) against *Candida albicans*. A, control .B, treated at concentration 62.5 $\mu\text{g/ml}$. C, treated at concentration 125 $\mu\text{g/ml}$. D, treated at concentration 250 $\mu\text{g/ml}$, E, treated at concentration 500 $\mu\text{g/ml}$

Conclusion

A number of new potent heterocyclic compounds that we successfully synthesized incorporating silver nanoparticles of tetrahydropyrimidine moiety; different spectral analysis methods have been used to corroborate the structures of the products. All compounds were examined in vitro for their antifungal and antibacterial properties against *C.albicans* and various strains of bacteria, with several derivatives exhibiting inhibitory zones that were comparable to those of the reference drug.

References

1. M. Priya, R. K. Selvan, B. Senthilkumar, M. K. Satheeshkumar, and C. Sanjeeviraja, "Synthesis and characterization of CdWO₄ nanocrystals," *Ceramics International*, vol. 2011 ; 37(7):2485–2488.

2. Akl M Awwad, Nidá M Salem and Amany O Abdeen. Green synthesis of silver nanoparticles using carob leaf extract and its antibacterial activity. *International Journal of Industrial Chemistry*. 2013; 4:29.
3. Alakbar E. Huseynzada, Christian Jelch, Haji Vahid N. Akhundzada, Sarra Soudani, Cherif Ben Nasr, Aygun Israyilova, Filippo Doria, Ulviyya A. Hasanova, Rana F. Khankishiyeva and Mauro Freccero. Synthesis, crystal structure and antibacterial studies of dihydropyrimidines and their regioselectively oxidized products. *RSC Adv*. 2021; 11:6312-6329.
4. Ali, I. H., Jabir, M. S., Al-Shmgani, H. S., Sulaiman, G. M., and Sadoon. Pathological And immunological study on infection with escherichia coli in ale balb/c mice. *Journal of Physics*. 2018, 1003(1), 12009.
5. Amritpal Kaura , Simran Preetb , Vivek Kumarc , Rajeev Kumard and Rajesh Kumar. Synergetic Effect of Vancomycin Loaded Silver Nanoparticles for Enhanced Antibacterial Activity. *Colloids and Surfaces B: Biointerfaces*. 2018.
6. Bahjat, H. H., Ismail, R. A., Sulaiman, G. M., and Jabir, M. S. Magnetic field-assisted laser ablation of titanium dioxide nanoparticles in water for antibacterial applications. *Journal of Inorganic and Organometallic Polymers and Materials*. 2021: 1-8.
7. Basavaraj Padmashali, Ballekere Nanjundaswamy Chidananda and Banuprakash Govindappa. Synthesis and characterization of novel 1,6-dihydropyrimidine derivatives for their pharmacological properties. 2019; 9(05): 133-140.
8. Bosshard, H. H.; Mory, R.; Schmid, M.; Zollinger, H. *Helv. "Advanced Organic Chemistry, Reaction Mechanisms; Harcourt/Academic: San Diego*. 2002; 239.
9. Chetan K. Jadhav, Amol S. Nipate, Asha V. Chate. Efficient Rapid Access to Biginelli for the Multicomponent Synthesis of 1,2,3,4-Tetrahydropyrimidines in Room-Temperature Diisopropyl Ethyl Ammonium Acetate. *ACS Omega*. 2019; 4:22313-22324.
10. El-Dash, Y.; Elzayat, E.; Abdou, A.M.; Hassan, R.A. Novel thienopyrimidine-aminothiazole hybrids: Design, synthesis, antimicrobial screening, anticancer activity, effects on cell cycle profile, caspase-3 mediated apoptosis and VEGFR-2 inhibition. *Bioorg. Chem*. 2021, 114, 105137.
11. Erum Dilshad, Mehmoona Bibi, Nadeem Ahmed Sheikh, Khairul Fikri Tamrin, Qaisar Mansoor, Qaisar Maqbool and Muhammad Nawaz. Synthesis of Functional Silver Nanoparticles and Microparticles with Modifiers and Evaluation of Their Antimicrobial, Anticancer, and Antioxidant Activity. *J. Funct. Biomater*. 2020; 11, 76.
12. Evanoff, D.D.; Chumanov, G. Size-controlled synthesis of nanoparticles. 2. Measurement of extinction, scattering, and absorption cross sections. *J. Phys. Chem. B*. 2004; 108:13957-13962.
13. Fissan, H.; Ristig, S.; Kaminski, H.; Asbach, C.; Eppele, M. Comparison of different characterization methods for nanoparticle dispersions before and after aerosolization. *Anal. Methods* 2014; 6:7324-7334.
14. Guyue Cheng, Menghong Dai , Saeed Ahmed, Haihong Hao, Xu Wang and Zonghui Yuan. Antimicrobial Drugs in Fighting against Antimicrobial Resistance, *Front. Microbiol*. 2016; 7:470.

15. Hnagarajiah, Imtiyaz Ahmed M. Khazi and Noor Shahina. Synthesis of some new derivatives of thiazolopyrimidines and hydrolysis of its arylidene derivative. 2015; 127(3): 467–479.
16. Jang, H.J.; Kim, S.M.; Rho, M.C.; Lee, S.W.; Song, Y.H. Synthesis of thienopyrimidine derivatives as inhibitors of STAT3 activation induced by IL-6. *J. Microbiol. Biotechnol.* 2019, 29, 856–862.
17. Jihad, M. A., Noori, F., Jabir, M. S., Albukhaty, S., AlMalki, F. A., and Alyamani, A. A. Polyethylene Glycol Functionalized Graphene Oxide Nanoparticles Loaded with *Nigella sativa* extract: A Smart Antibacterial Therapeutic Drug Delivery System. *Molecules.* 2021; 26(11), 3067.
18. Johal, M.S. *Understanding Nanomaterials*; CRC Press: Boca Raton, FL, USA, 2011.
19. Jose Vega-Baudrit, Stephanie Marin Gamboa, Ericka Rodriguez Rojas and Veronica Vega Martinez. Synthesis and characterization of silver nanoparticles and their application as an antibacterial agent. *International Journal of Biosensors & Bioelectronics.* 2019; 5(5):166-173.
20. Khashan, K. S., Abdulameer, F. A., Jabir, M. S., Hadi, A. A., and Sulaiman, G. M. Anticancer activity and toxicity of carbon nanoparticles produced by pulsed laser ablation of graphite in water. *Advances in Natural Sciences: Nanoscience and Nanotechnology.* 2021; 11(3), 035010.
21. Khashan, K. S., Badr, B. A., Sulaiman, G. M., Jabir, M. S., and Hussain, S. A. Antibacterial activity of Zinc Oxide nanostructured materials synthesis by laser ablation method. In *Journal of Physics: Conference Series.* 2021; 1795(1), 012040.
22. Kumar, B.; Smita, K.; Cumbal, L.; Debut, A. Green synthesis of silver nanoparticles using Andean blackberry fruit extract. *Saudi J. Biol. Sci.* 2017; 24:45–50.
23. Lin, P.C.; Lin, S.; Wang, P.C.; Sridhar, R. Techniques for physicochemical characterization of nanomaterials. *Biotechnol. Adv.* 2014; 32:711–726.
24. Mafaldo-Gómez, D. A., & Reyes-Meza, O. B. (2022). Training in values in environmental education in high school students: Case study: Education, environment, and society. *International Journal of Life Sciences*, 6(2), 65–71. <https://doi.org/10.53730/ijls.v6n2.10561>
25. Marambio-Jones, C.; Hoek, E.M.V. A review of the antibacterial effects of silver nanomaterials and potential implications for human health and the environment. *J. Nanopart. Res.* 2010; 12:1531–1551.
26. Marek K. Grzegorz S., Jerzy K., Szymon U., Mariusz B. , Tomasz B Aczek, A.S., Katarzyna S., Bernadeta S. , Gabriel N., Beata D., and Franciszek H. Synthesis of Novel Pyrido[1,2-c]pyrimidine Derivatives with 6-Fluoro-3-(4-piperidynyl)-1,2-benzisoxazole Moiety as Potential SSRI and 5-HT1A Receptor Ligands. *Int. J. Mol. Sci.* 2021; 22(5): 2329.
27. Martínez-Castañón, G.; Niño-Martínez, N.; Loyola-Rodríguez, J.; Patiño-Marín, N.; Martínez-Mendoza, J.; Ruiz, F. Synthesis of silver particles with different sizes and morphologies. *Mater. Lett.* 2009; 63:1266–1268.
28. Mohammed, M. K., Mohammad, M. R., Jabir, M. S., and Ahmed, D. S. Functionalization, characterization, and antibacterial activity of single wall and multi wall carbon nanotubes. In *IOP Conference Series: Materials Science and Engineering.* 2020; 757(1), 012028.
29. Olayinka O. Ajani, Fisayo E. Owolabi, Emmanuel G. Jolayemi, Oluwatosin Y. Audu and Olatunde M. Ogunleye. Facile synthesis of N'-(anthracen-9(10H)-

- ylidene)-4-(4- hydrophenyl)-6-methyl-2-oxo-1,2,3,4-tetra hydroypyrimidine-5-carbohydrazide and other derivate. *Journal of Physics: Conf. Series* 1299. 2019; 012116.
30. Prem Santhi Yerragopu1, Sharanagouda Hiregoudar1 and Udaykumar Nidon. Chemical Synthesis of Silver Nanoparticles Using Tri-sodium Citrate, Stability Study and Their Characterization. *International Research Journal of Pure & Applied Chemistry*. 2020; 21(3): 37-50.
 31. Rahmadeni, A. S. ., Hayat, N. ., Alba, A. D. ., Badri, I. A. ., & Fadhila, F. . (2020). The relationship of family social support with depression levels of elderly in 2019 . *International Journal of Health & Medical Sciences*, 3(1), 111-116. <https://doi.org/10.31295/ijhms.v3n1.188>
 32. Rana R, Sharma R, Kumar A. Repurposing of Existing Statin drugs for treatment of Microbial Infections: How much Promising? *Infect Disord DrugTargets*. 2018.
 33. Rostampour Esmail, Alihosseini Afshar, Milani Morteza, Akbarzadeh Abolfazl & Ebrahim Akhondi. Synthesis of silver nanoparticles with high efficiency and stability by culture supernatant of *Bacillus ROM6* isolated from Zarshouran gold mine and evaluating its antibacterial effects. *BMC Microbiology*. 2022; 22:97.
 34. Sayed K. Ramadan, Eman A. E. El-Helw and Hanan A. Sallam. Cytotoxic and antimicrobial activities of some novel heterocycles employing 6-(1,3-diphenyl-1H-pyrazol-4-yl)-4-oxo-2-thioxo-1,2,3,4-tetrahydropyrimidine-5-carbonitrile. *De Gruyter Heterocycl. Commun*. 2019; 25:107–115.
 35. Shabnam Pourmoslemi, Shirin Moradkhani, Pari Tamri and Sahar Foroughinia. Evaluation of synergistic antibacterial effect of combined *scrophularia striata* extract and antibiotics against *pseudomonas aeruginosa* and *Methicillin -Resistant Staphylococcus aureus*. *Iraqi J. Pharm. Sci*. 2021; 30(2) .
 36. Suryasa, I. W., Rodríguez-Gámez, M., & Koldoris, T. (2021). Get vaccinated when it is your turn and follow the local guidelines. *International Journal of Health Sciences*, 5(3), x-xv. <https://doi.org/10.53730/ijhs.v5n3.2938>
 37. Thi Thoi Bui1, Dai Quang Ngo and Van Loc Tran. Synthesis of sulfonylurea derivatives and their α -glucosidase inhibitory activity. *Vietnam journal of science, technology and engineering*. 2020; 62(2):34-37.
 38. Wang, Z.L. transmission electron microscopy of shape-controlled nanocrystals and their assemblies. *J. Phys. Chem. B*. 2000; 104:1153–1175.
 39. Wiley, B.; Sun, Y.; Mayers, B.; Xia, Y. Shape-controlled synthesis of metal nanostructures: The case of silver. *Chem. Eur. J*. 2005; 11:454–463.
 40. Yao, H.; Kimura, K. Field emission scanning electron microscopy for structural characterization of 3D gold nanoparticle super lattices. In *Modern Research and Educational Topics in Microscopy*; Méndez-Vilas, A., Díaz, J., Eds.; Formatex Research Center: Badajoz, Spain, 2007; 568–575.
 41. Younus, A., Al-Ahmer, S., and Jabir, M. Evaluation of some immunological markers in children with bacterial meningitis caused by *Streptococcus pneumonia*. *Research Journal of Biotechnology*. 2019; 14: 131-133.
 42. Zhuang, J.; Ma, S. Recent Development of pyrimidine-containing antimicrobial agents. *Chem Med Chem* 2020, 15, 1875–1886.